Research on Concentrated Solar Thermal Power Efficiency Based on Solar Elevation

Xiaomo Wang *

School of Automation, Central South University, ChangSha, China, 410083

* Corresponding Author Email: wangxiaomo0821@126.com

Abstract. This paper explores the impact of solar elevation on the reflective efficiency of heliostats in solar thermal power systems. By assuming heliostats as ideal mirrors and using detailed mathematical models, it calculates the cosine efficiency, shadow obstruction, and truncation efficiencies across different months. The study reveals how variations in solar elevation angles throughout the year affect the optimal tilt of heliostats, significantly impacting their efficiency. It also addresses the mutual shading and shadows cast by the absorber tower, proposing a model to estimate the obstructed area when heliostats are positioned vertically. The results highlight the necessity for precise positioning of heliostats to maximize solar capture and minimize losses, providing crucial insights for optimizing the layout of solar heliostat fields to enhance overall energy production and field efficiency. This research underscores the importance of strategic planning in the design of solar thermal power systems to adapt to seasonal changes in solar elevation.

Keywords: Solar elevation, Heliostat efficiency, Optical modeling, Solar thermal power.

1. Introduction

The development and optimization of solar thermal power systems are critical in the transition towards renewable energy sources[1]. Heliostats, which are mirrors designed to reflect sunlight onto a central receiver, play a pivotal role in the efficiency of these systems[2, 3]. The performance of heliostats is heavily influenced by several factors, including the angle of incoming sunlight, which varies with time of day, season, and geographical location[4]. Understanding the impact of solar elevation on the reflective efficiency of heliostats can significantly enhance their performance and, consequently, the overall efficiency of solar thermal power plants.

Previous studies have focused on the physical properties of heliostats and the mechanical aspects of their operation, but there is a need for more in-depth analysis on the optical efficiencies dictated by solar geometry[5, 6]. The elevation angle of the sun changes throughout the year due to the Earth's axial tilt and orbit, affecting the amount of solar energy a heliostat can capture and reflect[7]. This research aims to fill the gap by developing a comprehensive model that not only predicts heliostat performance based on solar elevation but also considers factors such as shadow obstruction and truncation efficiency, which have been less emphasized in existing literature.

By advancing the understanding of these dynamics, this study seeks to provide actionable insights that can be used to design better heliostat fields, optimizing their layout to reduce losses from shadows and enhance light capture. This research could lead to significant improvements in the cost-effectiveness and energy output of solar thermal power stations, making them a more viable option in the global energy mix.

2. Impact of Solar Elevation on Heliostat Reflective Efficiency

Because the Sun is far from the Earth and has a large size, when calculating sunlight exposure in practice, sunlight is considered as a conical beam of light with a relatively large apex angle[8]. Therefore, the angle of sunlight on the Earth in different seasons can be approximated as shown in the Figure 1:

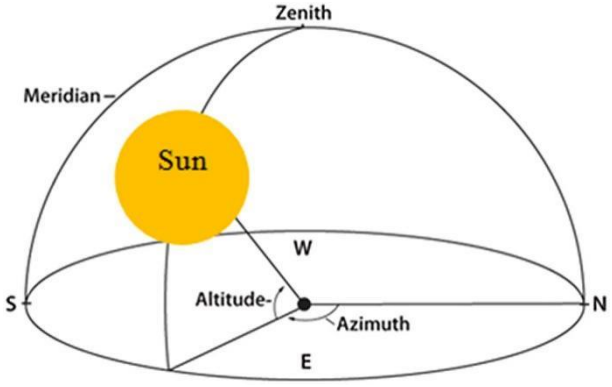

Figure 1: Schematic Diagram of the Sun's Position [9]

The image above shows the position of the sun at noon on different dates, from which the formula for calculating the solar elevation angle can be derived.

$$sin\,\alpha_s = cos\,\delta\,cos\,\varphi\,cos\,w + sin\,\delta\,sin\,\varphi \tag{1}$$

In the formula, φ represents the local latitude, with positive values for northern latitudes; w denotes the solar hour angle.

$$w = \frac{\pi}{12}(ST - 12) \tag{2}$$

In this context, ST refers to the local time, and δ represents the solar declination angle.

$$sin\,\delta = sin\frac{2\pi D}{365}\,sin\left(\frac{2\pi}{360}23{,}45\right) \tag{3}$$

Herein, D represents the number of days counted from the spring equinox, taken as day 0. For example, if the spring equinox is on March 21st, then April 1st corresponds to D=11.

Using equations 1-4, the solar elevation angles at different times on the 21st of each month are calculated as shown in the Table 1.

Table 1: Solar Elevation Angles at Different Times

Date	9:00	10:30	12:00	13:30	15:00
January 21	0.304227	0.474837	0.538151	0.474837	0.304227
February 21	0.433379	0.624353	0.697605	0.624353	0.433379
March 21	0.578066	0.79507	0.883137	0.79507	0.578066
April 21	0.725592	0.974851	1.08697	0.974851	0.725592
May 21	0.821146	1.095458	1.235592	1.095458	0.821146
June 21	0.853907	1.137361	1.29238	1.137361	0.853907
July 21	0.820053	1.094061	1.233763	1.094061	0.820053
August 21	0.719362	0.967106	1.077877	0.967106	0.719362
September 21	0.570265	0.785747	0.872862	0.785747	0.570265
October 21	0.41633	0.604491	0.676299	0.604491	0.41633
November 21	0.293727	0.462763	0.525352	0.462763	0.293727
December 21	0.251406	0.414187	0.473957	0.414187	0.251406

Building on this foundation, we begin to study the light reflection process using heliostats. Heliostats are optical devices that reflect sunlight onto a collector[10]. In practical applications, their reflective efficiency and accuracy vary due to factors such as material properties and operational lifespan. In this paper, they are considered as ideal mirrors, and the loss of light due to horizontal dispersion is not taken into account. This allows for the analysis of devices that adjust their vertical tilt solely in response to changes in the solar elevation angle, as illustrated in the Figure 2:

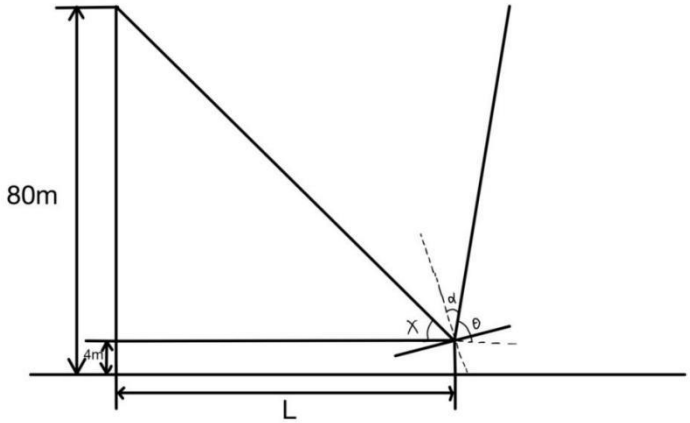

Figure 2: Schematic Diagram of Heliostat Reflection

In the diagram, L represents the distance from the center of each heliostat to the collector tower, while x and α denote angles, and θ represents the solar elevation angle. From these relationships, the following calculations can be derived:

$$\alpha = \frac{(\pi-\theta)-x}{2} \tag{4}$$

In the formula, $x = arctan\frac{80}{L}$. By substituting the solar elevation angles for different times on the 21st of each month into this equation, the angle α is obtained. The cosine of this angle then represents the cosine efficiency, as shown in the Table 2:

Table 2: Calculation results for cosine efficiency

Date	Cosine efficiency
January 21	0.3792
February 21	0.4441
March 21	0.5152
April 21	0.5860
May 21	0.6313
June 21	0.6468
July 21	0.6308
August 21	0.5831
September 21	0.5114
October 21	0.4357
November 21	0.3738
December 21	0.3523

3. Efficiency Modeling and Annual Energy Production in Solar Heliostat Fields

Due to the composition of the heliostat field consisting of multiple mirrors, there is potential for mutual shading among the mirrors. Additionally, the shadow cast by the absorber tower may block some of the mirrors from reflecting sunlight effectively. To address this, a model of the heliostat is proposed where all mirror surfaces are assumed to be positioned vertically, as illustrated below. This setup allows for the calculation of the area of the mirrors that is obstructed under these conditions.

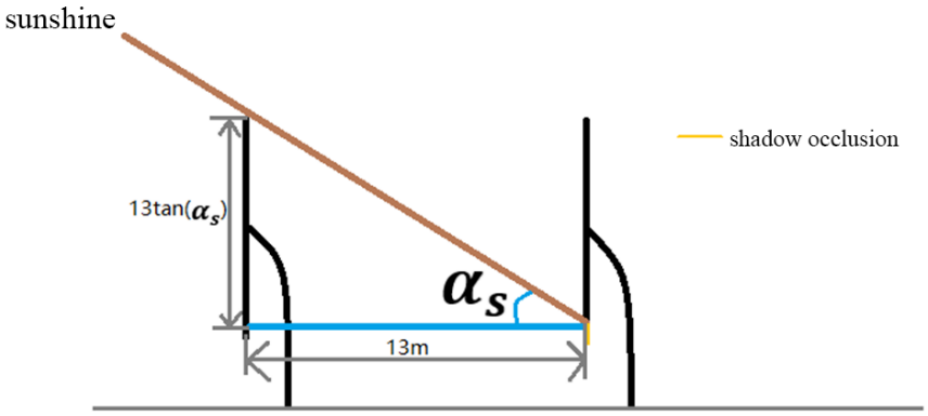

Figure 3: Schematic Diagram of Shadow Obstruction in Heliostats

As shown in Figure 3, α_s represents the solar elevation angle. Therefore, it can be determined that when all heliostats are in a vertical position, the shadow obstruction efficiency, denoted as η'_{sb}, is:

$$\eta'_{sb} = \frac{13\ tan\ \alpha_s}{6} \tag{5}$$

By inputting data, we can calculate the shadow obstruction efficiency for the heliostats in a vertical position on the 21st of each month.

Since it is impractical for the heliostats to be positioned vertically, using planar projection, it is known that when the tilt angle of the heliostats is θ, the shadow obstruction efficiency is:

$$\eta_{sb} = sin\ \bar{\theta} \cdot \eta'_{sb} \tag{6}$$

Here, $\bar{\theta}$ represents the annual average tilt angle of the heliostats. By substituting this value, we can determine the shadow obstruction efficiency due to mutual shading among the heliostats. Adding the efficiency loss caused by the shadow of the absorber tower gives us the total shadow obstruction efficiency.

Since not all of the light reflected by the heliostats is guaranteed to strike the receiver, there is an associated energy loss during the process of the receiver absorbing the reflected light. This proportion of energy loss is referred to as the receiver truncation efficiency. Additionally, since both the absorber tower and the receiver are cylindrical in shape, the range of light reflected by a single heliostat onto the receiver is depicted in the diagram below within a dashed frame. If the visible area of this light is unfolded, it forms a rectangle, the width of which is approximately calculated to be 5.89 meters.

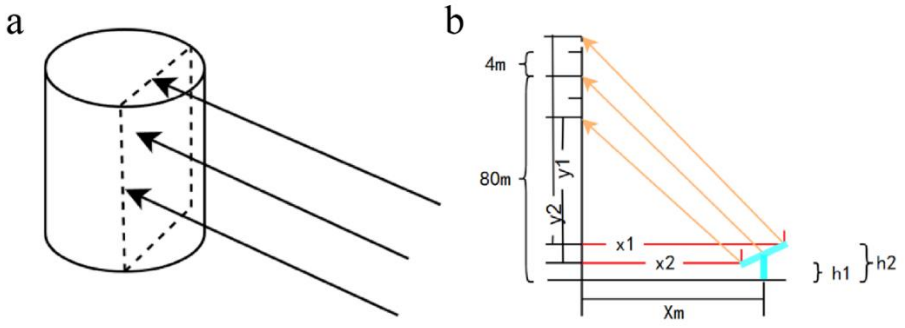

Figure 4: (a) Receiver Illumination Diagram; (b) Schematic Diagram for Calculating Truncation Efficiency

In Figure 4, x_1 and x_2 represent the distances from the upper and lower edges of the heliostat to the absorber tower, respectively. x_m represents the distance from the center of the heliostat to the ground.

$$x_1 = x_m - 3\ cos\ \theta \tag{7}$$

$$\chi_2 = x_m + 3\ cos\ \theta \tag{8}$$

y_1 and y_2 respectively represent the heights of the upper and lower edges of the light reflected by the heliostat on the absorber tower.

$$y_1 = x_1 \, tan\left(\frac{76}{x_m}\right) \tag{9}$$

$$y_2 = x_2 \tan\left(\frac{76}{x}\right) \tag{10}$$

h_1 and h_2 represent the distances from the ground to the upper and lower edges of the heliostat, respectively.

$$h_1 = 4 - 3 \, sin\,\theta \tag{11}$$

$$h_2 = 4 + 3 \, sin\,\theta \tag{12}$$

$$h_{min} = y_1 + h_1 \tag{13}$$

$$h_{\max} = y_2 + h_2 \tag{14}$$

The truncation efficiency of the receiver is defined as:

$$\eta_{truns} = \frac{Actual\ illuminated\ area}{Reflected\ light\ area\ from\ heliostat} \tag{15}$$

Atmospheric transmittance represents the loss of light as it passes through the atmosphere. In this context, it is assumed that the atmospheric transmittance is solely dependent on the path length of sunlight through the atmosphere, and the formula for its calculation is:

$$\eta_{at} = 0.99321 - 0.0001176 d_{HR} + 1.97 \times 10^{-8} \times d_{HR}^2 \tag{16}$$

Here, d_{HR} represents the distance from the center of the mirror to the center of the receiver. The reflectance of the mirror surface, η_{ref} is taken as a constant value of 0.92.

Thus, by calculating the cosine efficiency, shadow obstruction efficiency, truncation efficiency, and atmospheric transmittance for each 21st of the month at 9:00, 10:30, 12:00, 13:30, and 15:00, and averaging these, we can determine the average cosine efficiency, average shadow obstruction efficiency, and average truncation efficiency for that day. The formula for optical efficiency is:

$$\eta = \eta_{sb}\eta_{cos}\eta_{at}\eta_{trunc}\eta_{ref} \tag{17}$$

By multiplying the average cosine efficiency, average shadow obstruction efficiency, and average truncation efficiency for each month, we can obtain the average optical efficiency. The formula for calculating the thermal efficiency output of the heliostat field is:

$$E_{field} = DNl \cdot \sum_i^N A_i \, \eta_i \tag{18}$$

DNI (Direct Normal Irradiance) refers to the solar radiation energy received per unit area per unit time on a surface perpendicular to the sun's rays on Earth. It can be approximated using the following formula:

$$DNI = G_0 \left[a + b \, exp\left(-\frac{c}{sin\,\alpha_s}\right)\right] \tag{19}$$

$$a = 0.4237 - 0.00821(6 - H)^2 \tag{20}$$

$$b = 0.5055 - 0.00595(6.5 - H)^2 \tag{21}$$

$$a = 0.2711 - 0.01858(2.5 - H)^2 \tag{22}$$

Herein, G_0 represents the solar constant, which is valued at 1.366 kW/m², and H denotes the altitude in kilometers. Based on the above discussion, we can calculate the results as shown in Table 3.

Table 3: Average Optical Efficiency and Power Output on the 21st of Each Month

Date	Average optical efficiency	Average cosine efficiency	Average shadowing efficiency	Average truncation efficiency	Unit area mirror average output thermal power
January 21	0.032	0.3792	0.1979	0.4810	0.0321
February 21	0.0531	0.4441	0.2800	0.4811	0.0532
March 21	0.0870	0.5152	0.3941	0.4814	0.0870
April 21	0.1398	0.586	0.5568	0.4818	0.1398
May 21	0.1930	0.6313	0.7129	0.4822	0.1930
June 21	0.2173	0.6468	0.7831	0.4824	0.2172
July 21	0.1922	0.6308	0.7107	0.4822	0.1922
August 21	0.1370	0.5831	0.5484	0.4818	0.1370
September 21	0.0847	0.5114	0.3871	0.4814	0.0847
October 21	0.0500	0.4357	0.2683	0.4811	0.0500
November 21	0.0307	0.3738	0.1918	0.4810	0.0307
December 21	0.0253	0.3523	0.1677	0.4810	0.0253

The annual average thermal power output equals the product of the average thermal power output per unit area of the mirror surface, the area of a single heliostat, and the number of heliostats. The results are presented in the following table:

Table 4: Annual Average Optical Efficiency and Power Output Table

Annual Average Optical Efficiency	Annual Average Cosine Efficiency	Annual Average Shadow Obstruction Efficiency	Annual Average Truncation Efficiency	Annual Average Thermal Power Output (MW)	Average Thermal Power Output per Unit Mirror Area (kW/m^2)
0.1020	0.5005	0.4273	0.4749	6.3950	0.1021

4. Conclusions

This research develops an advanced model to accurately calculate and predict the performance of a heliostat field, taking into consideration the changes in solar elevation angle caused by the Earth's orbit and multiple optical efficiencies. Our findings highlight the significant impact of shadow obstruction, which accounts for a substantial portion of the solar radiation loss in the field. This result underscores the need for strategic planning in the layout and positioning of heliostats to mitigate shadowing effects and optimize the field's overall efficiency. The study provides a crucial foundation for enhancing the design of solar thermal power systems, aiming to maximize energy capture and minimize losses.

References

[1] POTRC S, CUCEK L, MARTIN M, et al. Sustainable renewable energy supply networks optimization–The gradual transition to a renewable energy system within the European Union by 2050[J]. Renewable and Sustainable Energy Reviews, 2021,146: 111186.

[2] RIZVI A A, DANISH S N, EL-LEATHY A, et al. A review and classification of layouts and optimization techniques used in design of heliostat fields in solar central receiver systems[J]. Solar Energy, 2021,218: 296-311.

[3] KANGOGO T K, KABINI K S. A Review of Heliostat Technologies used in Concentrated Solar Power Plants: Proceedings of the Sustainable Research and Innovation Conference[C], 2022.

[4] BHATTACHARJEE R, BHATTACHARJEE S. Performance of inclined heliostat solar field with solar geometrical factors[J]. Energy Sources, Part A: Recovery, Utilization, and Environmental Effects, 2020: 1-23.

[5] YERUDKAR A N, KUMAR D, DALVI V H, et al. Economically feasible solutions in concentrating solar power technology specifically for heliostats–A review[J]. Renewable and Sustainable Energy Reviews, 2024,189: 113825.

[6] ASHIKUZZAMAN A, SHAHRIAR M I, HASSAN M S. Optical Efficiency Analysis of Concentrated Solar Power Tower in Australia and Chile: Introduction and Optimization of Fractal Layout[J]. Available at SSRN 4237317.

[7] REDDY D S, KHAN M K. Stationary point focus solar concentrators—A review[J]. International Journal of Energy Research, 2022,46(5): 5678-5702.

[8] KAVUTHIMADATHIL S, RAMAMURTHY K. Location-specific optimization of free conic dome daylight collector for improved light pipe performance[J]. Building and Environment, 2024: 111497.

[9] AWASTHI A, SHUKLA A K, S. R. M M, et al. Review on sun tracking technology in solar PV system[J]. Energy Reports, 2020,6: 392-405.

[10] KURUP P, AKAR S, GLYNN S, et al. Cost update: commercial and advanced heliostat collectors[R]. National Renewable Energy Laboratory (NREL), Golden, CO (United States), 2022.